

# [Tetraphenylphosphonium](1+) {3,3'-*commo*-bis-[ $\eta^5$ -1,2-dicarba-(3)-nickel(III)-*clos*-dodecaborate]}(1-)-mono-tetrachloromethanate, [(C<sub>6</sub>H<sub>5</sub>)<sub>4</sub>P]<sup>+</sup>{Ni<sup>3+</sup>[ $\eta^5$ -(3)-1,2-B<sub>9</sub>C<sub>2</sub>H<sub>11</sub>]<sub>2</sub>}<sup>-</sup> · CCl<sub>4</sub>: Synthesis, Structure, and Temperature-Dependent EPR Spectra

T. M. Polyanskaya, V. A. Nadolniny, V. V. Volkov, and M. K. Drozdova

*Institute of Inorganic Chemistry, Siberian Division, Russian Academy of Sciences,  
pr. Akademika Lavrent'eva 3, Novosibirsk, 630090 Russia*

*E-mail: spectr@che.nsk.su*

Received July 18, 2007

**Abstract**—A novel compound containing tetraphenylphosphonium and nickel dicarbollyl, [[P(C<sub>6</sub>H<sub>5</sub>)<sub>4</sub>][Ni(B<sub>9</sub>C<sub>2</sub>H<sub>11</sub>)<sub>2</sub>] · CCl<sub>4</sub> (I) was synthesized and studied by X-ray diffraction and EPR methods. The crystals are monoclinic: C<sub>29</sub>H<sub>42</sub>B<sub>18</sub>PCl<sub>4</sub>Ni (*M* = 816.69), space group *P2/c*, the unit cell parameters *a* = 13.3964(5), *b* = 7.0556(2), *c* = 20.6610(8) Å,  $\beta$  = 94.9070(13)°, *V* = 1945.7(2) Å<sup>3</sup>, *Z* = 2,  $\rho$ (calcd.) = 1.394 g/cm<sup>3</sup>, *T* = 100 K, *F*(000) = 834,  $\mu$  = 0.081 mm<sup>-1</sup>. The structure was solved by the direct and Fourier methods and refined by the full-matrix least-squares method in the anisotropic (isotropic for the hydrogen atoms) approximation (*R*<sub>1</sub> = 0.032 for 4027 *I*<sub>hkl</sub> ≥ 2σ(*I*), 19886 measured and 5379 independent *I*<sub>hkl</sub>; X8 APEX Bruker diffractometer, λMoK $\alpha$ , graphite monochromator,  $\phi/\omega$  scan mode). At 100 K, the crystal contains the intermolecular hydrogen bonds B–H...Cl that favor the formation of infinite chains of the alternating anions and solvate molecules along the *z* axis of the unit cell. The single-crystal EPR study of complex I showed that the temperature changes of the cell parameters induce changes in the parameter of the *g*-factor *g*<sub>1</sub> directed along Cb–Ni–Cb. The cell parameters are increased and the *g*<sub>1</sub> value is gradually decreased with the increasing temperature. The temperature study of the EPR spectra of the powdered compound I revealed also jumpwise changes in *g*<sub>2</sub> and *g*<sub>3</sub> with hysteresis at 183–203 K depending on the direction of the temperature changes. The differences observed in the EPR spectra of the powders and single crystal of compound I in both the *g*-factor and the temperature dependence of its components are supposed to be caused by the CCl<sub>4</sub> vacancies formed in the crystal structure of a complex as a result of the partial removal of the solvate CCl<sub>4</sub> molecules when grinding the sample and by the change in the lability of the solvate molecules of a solvent with temperature.

DOI: 10.1134/S1070328408090078

The atoms, molecules, and ions are known to be involved in the complex interactions in compounds containing the hydrocarbon and hydride hydrogen atoms, the planar, cyclic, three-dimensional cluster aromatic (and even hyperaromatic) components, as well as the paramagnetic atoms are [1–4]. The above interactions change the structural, electronic, spectral, and the other physical properties of compounds. The title compound, [(C<sub>6</sub>H<sub>5</sub>)<sub>4</sub>P]<sup>+</sup>{Ni<sup>3+</sup>[ $\eta^5$ -(3)-1,2-B<sub>9</sub>C<sub>2</sub>H<sub>11</sub>]<sub>2</sub>}<sup>-</sup> · CCl<sub>4</sub> (I), which is the paramagnetic salt-like metal derivative of *ortho*-carborane(12), exhibits the above-mentioned complex interactions. The complex anion [NiCb<sub>2</sub>]<sup>-</sup> has a sandwich structure with the Ni(III) atoms coupled with two cluster ligands B<sub>9</sub>C<sub>2</sub>H<sub>11</sub><sup>2-</sup> (Cb), which have a three-dimensional aromaticity [3, 4]. The paramagnetic Ni(III) atom has the 3d<sup>7</sup> electronic configuration with *S* = 1/2 and realizes hypothetical C.N. 10. This config-

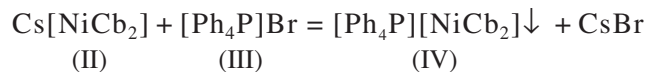
uration interacts with the electrons of two Cb ligands delocalized over the cluster atoms and enters their aromatic structure. Such systems with the delocalized electrons and hydride H atoms can interact with the planar benzoid aromatic fragments Ph of the [Ph<sub>4</sub>P]<sup>+</sup> cation, which should be followed by the structural and EPR changes of a complex.

This paper reports the synthesis, single-crystal X-ray diffraction and EPR study of the powder and single crystal of a novel complex I. One of the tasks of this work was to establish the reason for the temperature changes in the *g*-factor observed for the (NiCb<sub>2</sub>)<sup>-</sup> complexes with different cations.

## EXPERIMENTAL

**Synthesis.** The title compound I was synthesized as described in [4] by the precipitation of a bulky anion in

aqueous media (pH  $\approx$  4.5) with the  $[\text{Ph}_4\text{P}]^+$  cation according to the reaction



with subsequent filtration, drying, and recrystallization of the target product. The starting compound II was synthesized and identified by the known procedures [4, 5]. A weighed sample of compound III of the pure grade (0.184 g, 0.44 mmol) was dissolved in 200 ml of water at 70°C. Compound II (0.201 g, 0.44 mmol) was dissolved in 400 ml of hot water (70°C). Then, 50 ml of the acetate buffer solution (pH 4.56) and 0.05 g of  $\text{Na}_2\text{SO}_3$  (to suppress the  $\text{Ni}^{3+}$  oxidation) were added. In air, compound II is gradually oxidized in a solution to  $[\text{Ni}^{\text{IV}}\text{Cb}_2]^0$  insoluble in water. To remove the latter, the above solution of compound II was filtered and immediately poured to the stirred solution of III at 70°C. The light brown amorphous precipitate of  $[\text{Ph}_4\text{P}][\text{NiCb}_2]$  (IV) that formed was coagulated by the addition of  $\text{CaCl}_2$ . On cooling, the precipitate of IV was filtered, washed with water on the filter, dried in air, and in vacuum at room temperature to a constant weight. The yield of amorphous compound IV was 0.260 g (0.39 mmol, 89% as compared to II). Compound IV is soluble in acetone, acetonitrile, benzene, DMF, DMSO, THF,  $\text{CHCl}_3$ ,  $\text{CH}_2\text{Cl}_2$ , insoluble in  $\text{CCl}_4$ .

Crystals of I suitable for X-ray diffraction study were obtained by crystallization of IV dissolved in a mixture  $\text{CH}_2\text{Cl}_2$ – $\text{CCl}_4$ , on slow fractional evaporation at room temperature of a low-boiling  $\text{CH}_2\text{Cl}_2$  (*bp* 40.8°C).

**X-ray diffraction analysis** of crystals I was performed on the Bruker X8 APEX automated diffractometer at 100 K (Mo $K_\alpha$  radiation,  $\lambda = 0.71073$  Å, graphite monochromator,  $\phi/\omega$  scan mode at variable rate)[6]. The structure was solved by the direct method (SIR-97 [7]) combined with the Fourier syntheses. The coordinates, thermal parameters of non-hydrogen atoms, and the coefficient of isotropic extinction were refined with the SHELXL-97 program package [8] in isotropic and then, in anisotropic approximation by the full-matrix least-squares method (on  $F^2$ ). The positions of the hydrogen atoms were calculated geometrically and included in the refinement in the isotropic approximation with no restrictions.

The main crystallographic parameters of compound I, the summary of data collection and structure refinement are given in Table 1, the coordinates and equivalent isotropic thermal parameters of non-hydrogen atoms are listed in Table 2, the bond lengths and bond angles in the anion are presented in Table 3. The anisotropic thermal parameters, the coordinates of the hydrogen atoms, and tables of the structural factors are available from the authors.

The EPR spectra were recorded on a E-109 Varian automated spectrometer in the X-range of frequencies at 77-300 K and were modeled and analyzed with the WinEPR and Simfonia programs.

**Table 1.** The crystallographic parameters and summary of data collection and refinement of the  $[\text{P}(\text{C}_6\text{H}_5)_4][\text{Ni}(\text{B}_9\text{C}_2\text{H}_{11})_2] \cdot \text{CCl}_4$  structure

Parameter	Value
Empirical formula	$\text{C}_{29}\text{H}_{42}\text{B}_{18}\text{P}\text{Cl}_4\text{Ni}$
<i>M</i>	816.69
Crystal system	Monoclinic
Space group	<i>P2/c</i>
<i>a</i> , Å	13.3964(5)
<i>b</i> , Å	7.0556(2)
<i>c</i> , Å	20.6610(8)
$\beta$ , deg	94.9070(13)
<i>V</i> , Å <sup>3</sup>	1945.71(12)
<i>Z</i>	2
$\rho$ (calcd.), g/cm <sup>3</sup>	1.394
$\mu$ , mm <sup>-1</sup>	0.840
<i>F</i> (000)	834
Crystal size, mm	0.047 × 0.089 × 0.754
Range of $\theta$ , deg	1.53–31.78
Range of reflection indices	$-19 \leq h \leq 19, -5 \leq k \leq 10, -29 \leq l \leq 29$
Measured reflections	18869
Independent reflections	5379 ( $R_{\text{int}} = 0.0313$ )
Reflections with $I \geq 2\sigma(I)$	4027
Number of refined parameters	327
GOOF on $F^2$	1.104
<i>R</i> -factor ( $I > 2\sigma(I)$ )	$R_1 = 0.0322, wR_2 = 0.0757$
<i>R</i> -factor (for all reflections)	$R_1 = 0.0570, wR_2 = 0.0982$
Extinction coefficient	0.0012(5)
$\Delta\rho_{\text{max}}$ and $\Delta\rho_{\text{min}}$ , e Å <sup>-3</sup>	0.502 and -0.464

## RESULTS AND DISCUSSION

Compound I occurs as brown crystals. Its crystal structure is built of the tetraphenylphosphonium cations ( $\text{PPh}_4$ )<sup>+</sup> (on axes 2), the centrosymmetric nickel dicarbollyl anions  $\text{Ni}(\text{Cb}_2)^-$ , and the solvate tetrachloromethane molecules  $\text{CCl}_4$  (on axes 2) in a ration 1 : 1 : 1.

The structure of the  $[\text{Ni}(\text{B}_9\text{C}_2\text{H}_{11})_2]^-$  anion in I with atomic numbering is shown in Fig. 1.

The cation has common geometry. The P atom has a distorted tetrahedral coordination (P–C 1.794(2) Å, the CPC angles 106.2(1)°–111.2(1)°). The C–C, C–H bond lengths and CCC angles in the phenyl rings lie in the intervals 1.379(3)–1.404(3), 0.86(2)–0.94(3) Å and 119.5(2)°–120.4(2)°, respectively. The phenyl rings are planar  $\pm 0.003$ – $0.005$  Å).

The anion has the form of two icosahedra with a shared vertex, i.e., the Ni(III) atom. In the anions, two planes  $\{\text{C}_2\text{B}_3\}$  are bonded with the Ni atom according to the  $\eta^5$ -type and determine the conventional pentago-

**Table 2.** The coordinates ( $\times 10^4$ ) and equivalent isotropic thermal parameters  $U_{\text{eq}} = 1/3(U_{11} + U_{22} + U_{33}) (\times 10^3)$  of basic atoms in  $[\text{P}(\text{C}_6\text{H}_5)_4][\text{Ni}(\text{B}_9\text{C}_2\text{H}_{11})_2] \cdot \text{CCl}_4$ 

Atom	<i>x</i>	<i>y</i>	<i>z</i>	$U_{\text{eq}}, \text{\AA}^2$	Atom	<i>x</i>	<i>y</i>	<i>z</i>	$U_{\text{eq}}, \text{\AA}^2$
Ni	10000	0	0	10(1)	B(1)	7177(2)	-1390(3)	259(1)	17(1)
P	5000	-48(1)	2500	12(1)	B(2)	7872(2)	289(3)	763(1)	15(1)
C(1)	6010(1)	-1547(3)	2814(1)	14(1)	B(3)	7447(2)	850(3)	-49(1)	16(1)
C(2)	5812(2)	-2908(3)	3281(1)	17(1)	B(4)	7636(2)	-1185(3)	-526(1)	17(1)
C(3)	6573(2)	-4086(3)	3539(1)	19(1)	B(5)	8053(2)	-3079(3)	3(1)	17(1)
C(4)	7527(2)	-3935(3)	3329(1)	20(1)	B(6)	8203(2)	-2163(3)	799(1)	17(1)
C(5)	7724(2)	-2616(3)	2858(1)	20(1)	C(7A)	8653(1)	1300(3)	276(1)	13(1)
C(6)	6968(2)	-1415(3)	2598(1)	16(1)	C(8A)	8528(1)	487(3)	-434(1)	14(1)
C(7)	5407(1)	1478(3)	1880(1)	14(1)	B(9)	8933(2)	-1868(3)	-456(1)	15(1)
C(8)	5050(2)	1330(3)	1229(1)	17(1)	B(10)	9275(2)	-2527(3)	362(1)	15(1)
C(9)	5378(2)	2609(3)	781(1)	21(1)	B(11)	9168(2)	-398(3)	813(1)	14(1)
C(10)	6063(2)	4004(3)	977(1)	22(1)	C(13)	10000	3268(4)	2500	19(1)
C(11)	6427(2)	4147(3)	1627(1)	21(1)	Cl(1)	10308(1)	4715(1)	3183(1)	26(1)
C(12)	6097(2)	2906(3)	2078(1)	18(1)	Cl(2)	8959(1)	1828(1)	2633(1)	26(1)

nal-antiprismatic coordination of a central atom. The pairs of the atoms C-C of the dicarbollide ligands have the *trans*-positions in the parallel root-mean-square planes specified by two pentagonal  $\{\text{C}_2\text{B}_3\}$  faces. The Ni atom lies at 1.555 Å away from them. Five atoms of  $\{\text{C}_2\text{B}_3\}$  in a face are not coplanar i.e., the face is bent along the B(10)⋯B(11) line and has the envelope conformation with dihedral angle ( $\varphi$ ) equal to 6.3°. The low pentagonal belt B(2)–B(3)–B(4)–B(5)–B(6) is also bent along the B(2)⋯B(4) line in the envelope conformation ( $\varphi = 6.0^\circ$ ). The maximum deviations from the mean-square plane  $\{\text{C}_2\text{B}_3\}$  are equal to 0.046 Å for B(10) and 0.040 Å for B(11). The angle  $\varphi$  between the pentagonal belts in every icosahedral fragment of the ligands  $[\text{7,8-B}_9\text{C}_2\text{H}_{11}]^{2-}$  equals 1.6°. Note that two Ni–B bonds are likely to be stronger as compared to the Ni–C bonds (Ni(1)–B(9) 2.107(2), Ni(1)–B(11) 2.113(2), Ni(1)–C(8A) 2.124(2), Ni(1)–C(7A) 2.144(2) Å). On the whole, the distances between the Ni atoms and the coordinating atoms of the carborane ligand lie in the range 2.107(2)–2.193(2) Å. This fact agrees with a common notion that in the electron-saturated metallo-carboranes, the M–B bonds are strengthened due to the M–C bonds [9]. In the  $\text{B}_9\text{C}_2$  cluster, the distances C–C 1.571(3), B–B 1.752(3)–1.797(3), B–C 1.673(3)–1.750(3), B–H 1.03(2)–1.12(3), C–H 0.90(3)–0.92(2) Å.

The C–Cl bonds and ClCCl angles in the  $\text{CCl}_4$  molecule lie within the range 1.763(2)–1.766(2) Å and 108.91(3)°–110.03(3)°, respectively.

The shortest distance Ni⋯Ni in I (7.0556 Å) corresponds to the shortest spacing of the unit cell.

The projection of the crystal structure I on the (010) plane is presented in Fig. 2.

The comparison with the data obtained at room temperature indicates a ~3.3% decrease in the unit cell volume of crystal I at 100 K.

When the recording room temperature is decreased to 100 K, the following changes are observed in the anion:

- 1) the central Ni atom approaches two  $\{\text{C}_2\text{B}_3\}$  planes by ~0.01 Å (from 1.564 to 1.555 Å);
- 2) the  $\{\text{C}_2\text{B}_3\}$  bent is increased as that of the lower pentagonal  $\{\text{B}_5\}$  belt (from 2.7° and 2.5° to 6.3° and 6.0°, respectively);
- 3) the electron density redistribution in the  $\{\text{C}_2\text{B}_3\}$  planes is likely to occur, as a result of which the C atoms in the  $-\text{C}_2-$  groups approach one another by ~0.06 Å (from 1.632 to 1.571 Å) and, in addition, the observed strengthening of the Ni–B bonds as compared to Ni–C at 100 K has some other nature;
- 4) the Ni atoms approach one another by 0.092 Å (from 7.1475 to 7.0556 Å), the central atom of the sol-

**Table 3.** The main bond lengths and bond angles in the  $[\text{Ni}(\text{B}_9\text{C}_2\text{H}_{11})_2]^-$  anion of compound I

Bond	<i>d</i> , Å	Bond	<i>d</i> , Å	Bond	<i>d</i> , Å
Ni–B(9)	2.107(2)	B(2)–C(7A)	1.673(3)	B(5)–B(6)	1.764(3)
Ni–B(11)	2.113(2)	B(2)–B(3)	1.769(3)	B(5)–B(10)	1.782(3)
Ni–C(8A)	2.1237(19)	B(2)–B(6)	1.786(3)	B(5)–B(9)	1.792(3)
Ni–C(7A)	2.1443(19)	B(2)–B(11)	1.797(3)	B(6)–B(10)	1.779(3)
Ni–B(10)	2.193(2)	B(3)–C(7A)	1.725(3)	B(6)–B(11)	1.794(3)
B(1)–B(3)	1.752(3)	B(3)–C(8A)	1.731(3)	C(7A)–C(8A)	1.571(3)
B(1)–B(6)	1.780(3)	B(3)–B(4)	1.773(3)	C(7A)–B(11)	1.736(3)
B(1)–B(5)	1.784(3)	B(4)–C(8A)	1.678(3)	C(8A)–B(9)	1.750(3)
B(1)–B(2)	1.786(3)	B(4)–B(5)	1.785(3)	B(9)–B(10)	1.775(3)
B(1)–B(4)	1.788(3)	B(4)–B(9)	1.797(3)	B(10)–B(11)	1.780(3)
Angle	$\omega$ , deg	Angle	$\omega$ , deg	Angle	$\omega$ , deg
B(3)B(1)B(6)	109.37(16)	C(7A)B(3)B(2)	57.21(12)	B(6)B(5)B(9)	106.96(16)
B(3)B(1)B(5)	109.51(16)	C(8A)B(3)B(2)	100.91(15)	B(10)B(5)B(9)	59.58(12)
B(6)B(1)B(5)	59.32(13)	B(1)B(3)B(2)	60.94(13)	B(1)B(5)B(9)	108.53(16)
B(3)B(1)B(2)	59.98(13)	C(7A)B(3)B(4)	101.02(15)	B(4)B(5)B(9)	60.31(13)
B(6)B(1)B(2)	60.11(13)	C(8A)B(3)B(4)	57.21(12)	B(5)B(6)B(10)	60.37(13)
B(5)B(1)B(2)	107.05(15)	B(1)B(3)B(4)	60.96(14)	B(5)B(6)B(1)	60.43(13)
B(3)B(1)B(4)	60.09(13)	B(2)B(3)B(4)	107.24(16)	B(10)B(6)B(1)	109.79(16)
B(6)B(1)B(4)	106.67(16)	C(8A)B(4)B(3)	60.13(13)	B(5)B(6)B(2)	107.91(16)
B(5)B(1)B(4)	59.95(13)	C(8A)B(4)B(5)	105.97(15)	B(10)B(6)B(2)	109.07(16)
B(2)B(1)B(4)	105.84(16)	B(3)B(4)B(5)	108.54(16)	B(1)B(6)B(2)	60.09(13)
C(7A)B(2)B(3)	60.08(12)	C(8A)B(4)B(1)	104.55(16)	B(5)B(6)B(11)	107.06(16)
C(7A)B(2)B(1)	104.67(16)	B(3)B(4)B(1)	58.95(13)	B(10)B(6)B(11)	59.75(12)
B(3)B(2)B(1)	59.08(13)	B(5)B(4)B(1)	59.89(13)	B(1)B(6)B(11)	108.28(16)
C(7A)B(2)B(6)	105.82(16)	C(8A)B(4)B(9)	60.36(12)	B(2)B(6)B(11)	60.27(13)
B(3)B(2)B(6)	108.39(16)	B(3)B(4)B(9)	110.86(16)	C(8A)C(7A)B(2)	112.58(16)
B(1)B(2)B(6)	59.80(13)	B(5)B(4)B(9)	60.05(13)	C(8A)C(7A)B(3)	63.17(13)
C(7A)B(2)B(11)	59.90(12)	B(1)B(4)B(9)	108.11(16)	B(2)C(7A)B(3)	62.71(13)
B(3)B(2)B(11)	110.24(15)	B(6)B(5)B(10)	60.25(13)	C(8A)C(7A)B(11)	110.49(15)
B(1)B(2)B(11)	107.90(16)	B(6)B(5)B(1)	60.25(13)	B(2)C(7A)B(11)	63.60(13)
B(6)B(2)B(11)	60.08(12)	B(10)B(5)B(1)	109.54(16)	B(3)C(7A)B(11)	115.40(15)
C(7A)B(3)C(8A)	54.06(11)	B(6)B(5)B(4)	107.55(16)	C(7A)C(8A)B(4)	112.36(16)
C(7A)B(3)B(1)	103.93(15)	B(10)B(5)B(4)	108.63(16)	C(7A)C(8A)B(3)	62.77(13)
C(8A)B(3)B(1)	103.87(16)	B(1)B(5)B(4)	60.15(13)	B(4)C(8A)B(3)	62.65(13)
C(7A)C(8A)B(9)	111.26(15)	B(10)B(9)B(4)	108.36(16)	B(9)B(10)B(11)	104.58(15)
B(4)C(8A)B(9)	63.18(13)	B(5)B(9)B(4)	59.64(13)	C(7A)B(11)B(10)	107.04(15)
B(3)C(8A)B(9)	115.23(15)	B(5)B(10)B(6)	59.38(13)	C(7A)B(11)B(6)	102.87(15)
C(8A)B(9)B(10)	106.21(15)	B(5)B(10)B(9)	60.51(13)	B(10)B(11)B(6)	59.72(13)
C(8A)B(9)B(5)	102.66(15)	B(6)B(10)B(9)	107.01(15)	C(7A)B(11)B(2)	56.50(12)
B(10)B(9)B(5)	59.91(13)	B(5)B(10)B(11)	106.90(16)	B(10)B(11)B(2)	108.53(16)
C(8A)B(9)B(4)	56.45(12)	B(6)B(10)B(11)	60.53(13)	B(6)B(11)B(2)	59.64(13)

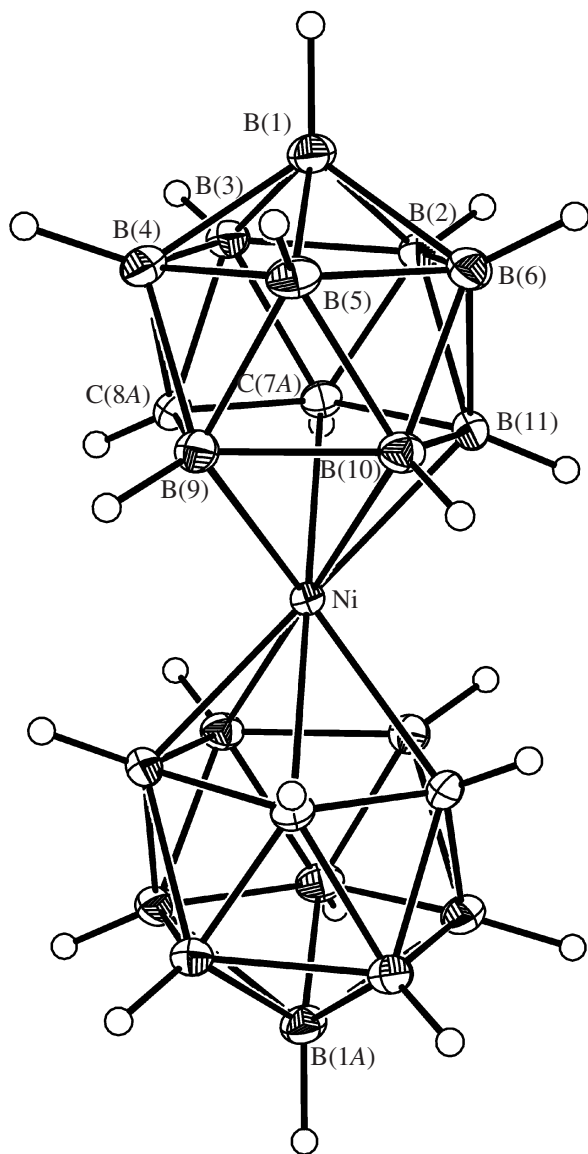


**Fig. 1.** The structure of the  $[\text{Ni}(\text{B}_9\text{C}_2\text{H}_{11})_2]^-$  anion in crystal I with atomic numbering (thermal displacement ellipsoids—50% probability).

vate molecule approaches the metal atom by  $\sim 0.05$  Å (from 5.706 to 5.656 Å), the central atom of the phosphorus cation approaches by 0.124 Å (from 8.225 to 8.101 Å);

5) the shortened contact between the Cl(10 atom and the hydride atom H(6B) of the anion ( $\text{Cl}\cdots\text{H}$  2.91 Å) is less than the sum of the van der Waals radii of the atoms Cl and H, which evidences the formation of hydrogen bonds  $\text{B}(6)\text{—H}(6\text{B})\cdots\text{Cl}(1)$  by which the alternating anions and the solvate molecules are united into infinite chains along the axis  $z$ .

The synthesized compound I represented concretion of the crystals or small crystals and therefore, was preliminarily ground in the agate mortar until the EPR spectra did not exhibit randomly oriented large fragments of the crystalline phase. The temperature dependence of the line width and the  $g$ -factor was obtained on increasing the temperature at a step of  $10^\circ$  from 123 to 273 K (with the accuracy of the temperature measurement  $\pm 1$ ). The EPR spectrum of the powdered compound I at 123 K has the form typical of the powdered sample with the anisotropic axial  $g$ -factor:  $g_1 = 2.093$ ,  $g_2 = 2.0064$ ,  $g_3 = 1.998$  (Fig. 3).

The width of the EPR lines increased considerably with the temperature, the increase in the width of each component obeying its own law (Fig. 4). The analysis of the line width of every component  $\Delta H$  shows that their temperature dependence is described by the expression

$$\Delta H = \alpha T + \beta T^7$$

with different parameters  $\alpha$  and  $\beta$  for every spectral component. Such a dependence is typical for the transition metal ions and is determined by the temperature dependence of the spin-lattice relaxation, which, in turn, suggests gradual freezing out of the lattice vibrations of different symmetry [10]. The modeling and analysis of the EPR spectrum shows that in the interval 123–263 K, the component of the  $g$ -factor  $g_1$  is gradually decreased. The temperature dependence of the components of the  $g$ -factor for the powdered sample is shown in Fig. 5. In the range of 183–203 K, the components  $g_3$  and  $g_2$  change in steps from 1.998 to 2.005 and from 2.012 to 2.019, respectively. The above changes in the  $g$ -factor with temperature are characteristic of the phase transitions. Therefore, the EPR spectra were studied with lowering the temperature from 253 to 123 K and then with raising the temperature from 123 to 253 K. In this case, hysteresis is observed for the component  $g_2$  in the region of a jumpwise change. The values of the component  $g_1$  also depend on the direction of the temperature changes, but it does not exhibit the hysteresis type of the changes. The jump in the change of the  $g_3$  component is observed for both decreasing and increasing temperatures.

As follows from the analysis of the  $g$ -factors of the analogous complexes [3, 11], the maximum value of the component  $g_1$  is determined to a greater extent by the interaction of the nickel ion with the sandwich structure of the complex, while the other two components change due to the effect of the close surrounding of the  $(\text{NiCb}_2)^-$  anion of the complex on the electron density distribution.

To refine the parameters of the EPR spectra, the additional study of single crystals of I grown from a solution in a mixture of the solvents  $\text{CCl}_4$  and  $\text{CH}_2\text{Cl}_2$  was performed. The angular dependence of the EPR spectrum on rotation of a crystal about the axis  $y$  in a plane passing through the crystal axes  $x$  and  $z$  is shown in Fig. 6. One can see that the paramagnetic complex

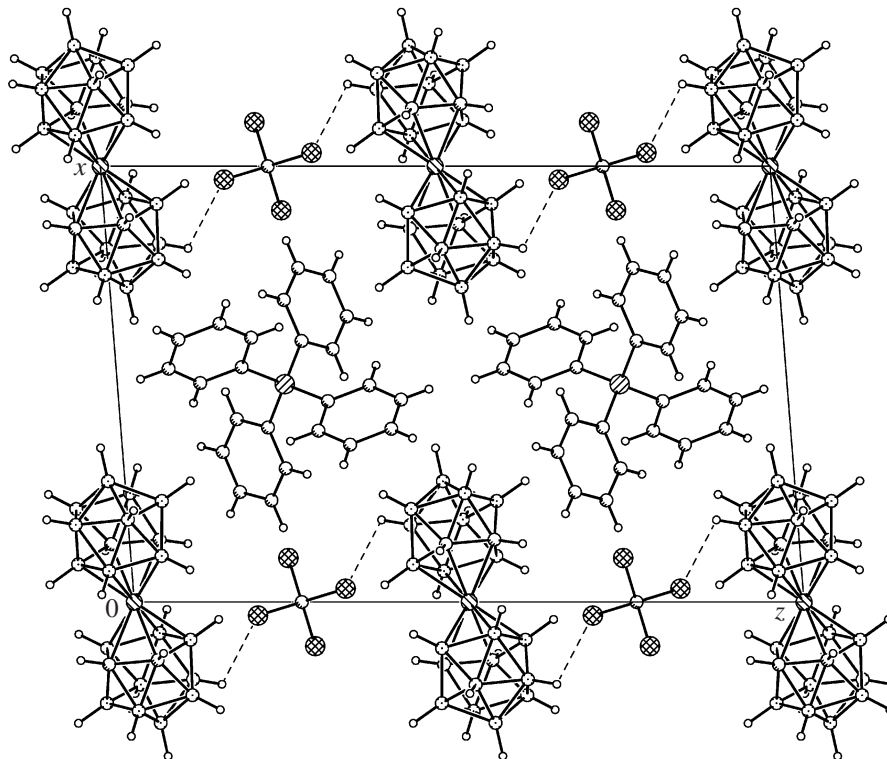


Fig. 2. The structural unit packing in crystal I, the projection along the direction [010].

has one magnetically nonequivalent position in the structure of a crystal, which correspond to the low crystal symmetry. On rotation in this plane at 123 K, the EPR spectra with the minimum (1.993) and maximum (2.093)  $g$ -factors are observed. The third value of the  $g$ -factor ( $g_2 = 2.0064$ ) was obtained from the angular dependence of the spectrum at  $H \parallel y$ . The powder and single crystal have equal  $g_1$  components. The slight dif-

ference in the  $g_2$  and  $g_3$  components can be explained by a partial loss of a solvent during crystal grinding or by the effect of the strains at the developed surface for the powders. The value and direction of  $g_1 = 2.093$  cor-

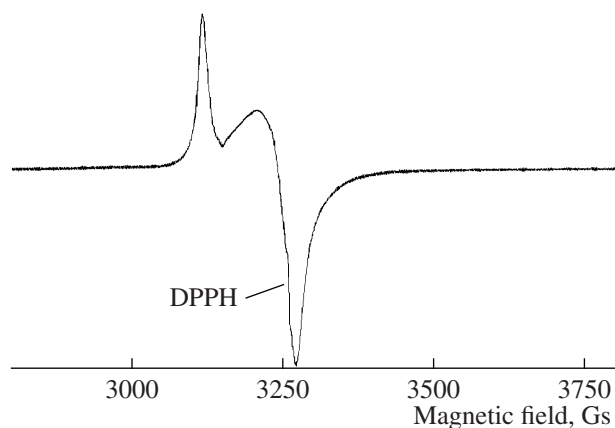


Fig. 3. The EPR spectrum of the powdered compound I at 123 K.

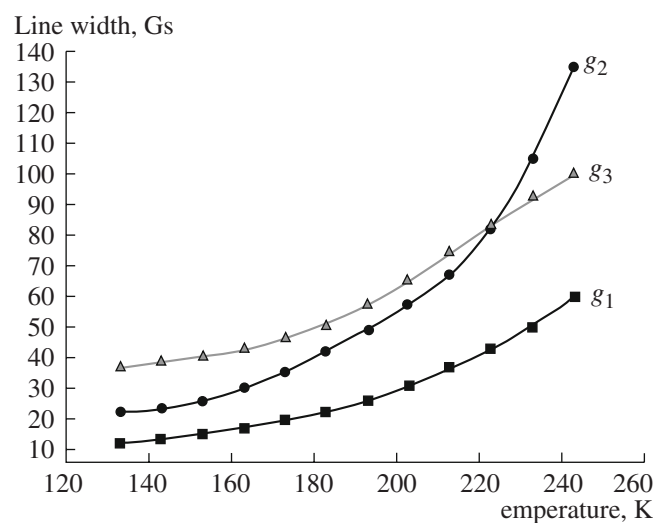
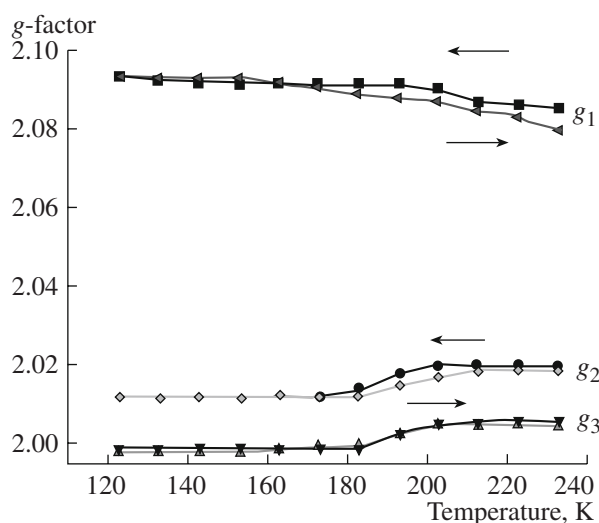


Fig. 4. The temperature dependence of the line width for different components of the EPR spectrum of the powdered compound I.



**Fig. 5.** The temperature dependence of the  $g$ -factor components for the powdered compound I (the direction of the temperature change is shown by arrows).

responds to the Cb–Ni–Cb (or B(1)Ni–B(1A) direction (Fig. 1).

The study of the temperature dependence of the  $g$ -factors for crystal I indicates that as in the case of the powders, the  $g_1$  component gradually decreases with the increasing temperature (Fig. 7) Unlike the powders, the  $g_2$  and  $g_3$  values in the crystal are independent of the temperature and equal to 2.0064 and 1.993, respectively.

The X-ray diffraction study reveals that the temperature increase (from 100 to 293 K) is attended by a noticeable increase in the distances between the nickel ion and the nearest atoms of icosahedra. Such a change in the structural parameters decreases the component of

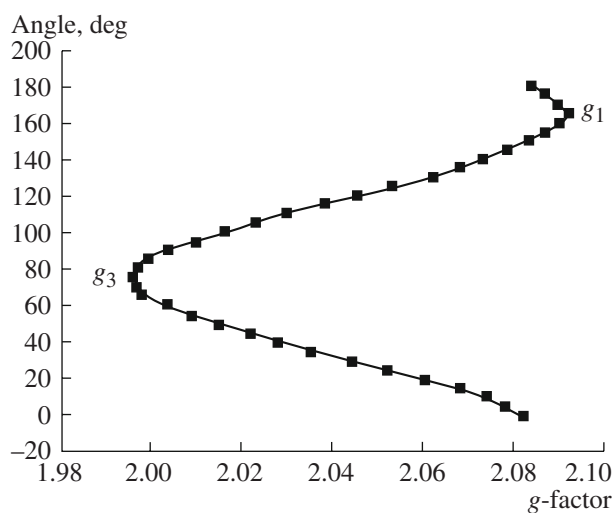


**Fig. 6.** The angular dependence of the EPR spectra of compound I in the  $xz$  plane of a crystal.

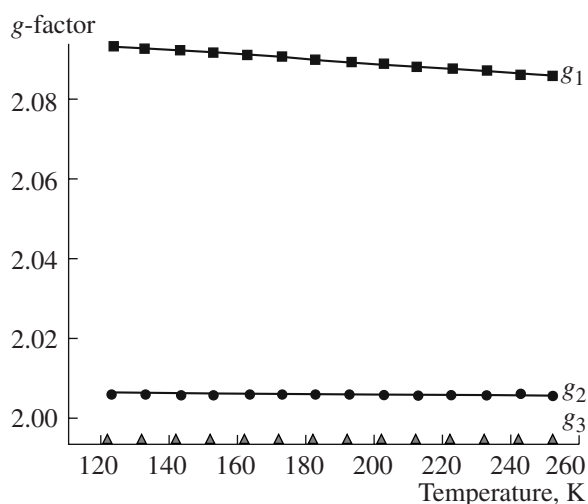


**Fig. 7.** The temperature dependence of the  $g$ -factor components for crystal I.

the  $g$ -factor along the Cb–Ni–Cb (or B(1)–Ni–B(1A)) direction. The above tendency is typical of both single crystals and powders. The crystal of complex I under consideration contains also the  $\text{CCl}_4$  molecules. Therefore, the weakening of the  $\text{Cl}\cdots\text{H}$  bond with the hydrogen atoms of the anion observed at room temperature on the basis of the X-ray diffraction data should also affect the electron density redistribution mainly in both icosahedra and the  $g_1$  component. According to the data in [3, 11], the perpendicular components of the  $g$ -factor are mainly influenced by the cation and by the electron density redistribution in the cationic part of a complex. As follows from the temperature dependence of the  $g$ -factors of a crystal, the components  $g_2$  and  $g_3$  remain unchanged. The temperature dependences of the EPR spectra of the powder and crystal differ in a larger width of the spectral lines for the  $g$ -factor components and in a jumpwise change in  $g_2$  and  $g_3$  for the powder, which depend on the nearest surrounding of the anionic part of the complex. The above temperature behavior of the  $g$ -factor can be explained by a higher lability of the solvent molecules in complex I for the powders due to the vacancies for the solvent molecules formed as a result of their partial removal during the sample grinding. As the temperature is decreased below 183 K, the solvate molecule  $\text{CCl}_4$  is stabilized in one of these vacant positions. The changes occurring in the nearest surrounding of the  $(\text{NiCb}_2)^-$  anion for the powder are confirmed by the changes in the  $g_2$ - and  $g_3$ -factors that differ somewhat from those for the crystal.

#### ACKNOWLEDGMENTS

The authors are grateful to E.V. Peresyphkina and A.V. Virovets for performing X-ray diffraction experiments.

## REFERENCES

1. Virovets, A.V., Vakulenko, N.N., Volkov, V.V., and Podberezskaya, N.V., *Zh. Strukt. Khim.*, 1994, vol. 35, no. 3, p. 72.
2. Varnek, V.A. and Volkov, V.V., *Zh. Strukt. Khim.*, 1995, vol. 36, no. 4, p. 709.
3. Nadolinny, V.A., Polyanskaya, T.M., Volkov, V.V., et al., *Koord. Khim.*, 2005, vol. 31, no. 6, p. 403 [*Russ. J. Coord. Chem.* (Engl. Transl.), vol. 31, no. 6, p. 379].
4. Volkov, V.V., Il'inchik, E.A., Kolesov, B.A., et al., *Zh. Strukt. Khim.*, 1996, vol. 37, no. 6, p. 1060.
5. Hawthorne, M.F., Young, D.C., Andrews, T.D., et al., *J. Am. Chem. Soc.*, 1968, vol. 90, no. 4, p. 879.
6. *APEX2 (Version 1.08), SAINT (Version 7.03) and SADABS (Version 2.11). Bruker Advanced X-ray Solutions*, Madison (WI, USA): Bruker AXS Inc., 2004
7. Altomare, A., Burla, M.C., Camalli, M., et al., *J. Appl. Crystallogr.*, 1999, vol. 32, p. 115.
8. Sheldrick, G.M., *SHELXL-97. Release 97-2*, Göttingen (Germany): Univ. of Göttingen, 1998.
9. Polyanskaya, T.M., Nadolinnyi, V.A., Volkov, V.V., et al., *Zh. Strukt. Khim.*, 2006, vol. 47, no. 5, p. 905.
10. Abragam, A. and Bleaney, B. *Electron Paramagnetic Resonance of Transition Ions*, Oxford: Clarendon, 1970, vol. 1.
11. Robertson, R.E. and McConnell, H.M., *J. Phys. Chem.*, 1960, vol. 64, no. 1, p. 70.